EFFECTS OF LOADING HISTORY ON CYCLIC PERFORMANCE OF STEEL RBS MOMENT CONNECTIONS

C M UANG[1], Q S YU[2] And C S GILTON[3]

SUMMARY

The cyclic response of steel reduced beam section moment connections under various loading histories was investigated. Four full-scale specimens were tested to failure, two using a standard loading protocol and two using a near-fault loading protocol. Each specimen experienced yielding in both the panel zone and the reduced beam section, with most of the plastic rotation occurring in the beam. Overall, the four specimens performed very well. No weld fractures were observed and they each reached a plastic rotation of 0.03 radian. The specimens tested with the near-fault loading protocol were able to reach 0.05 radian plastic rotation and could have reached more. The energy dissipation capacities of the four specimens were about the same.

INTRODUCTION

Widespread damage to steel moment frame structures during the 1994 Northridge earthquake led researchers to develop alternative connection designs to the prescriptive pre-Northridge moment connection. One such design, the reduced beam section (RBS), allows stable yielding of the beam and column panel zone by moving the plastic hinge region in the beam a short distance from the column face, protecting the beam flange groove welds from brittle fracture.

There has been previous testing of the RBS moment connection [Chen, 1996; Engelhardt et al,1998; Plumier, 1997; Zekioglu et al, 1997] which heralds the effectiveness of the new design in the post-Northridge design era. All of this testing, however, has been conducted using standard loading protocols. Recently, questions have arisen concerning the effects of an earthquake occurring in the immediate vicinity of a structure. Earthquake engineering is in need of the testing of the RBS moment connection using the so-called near-fault loading protocol.

OBJECTIVE

The main objective of this research was to investigate the cyclic response of the steel RBS moment connection under various loading histories. Comparisons were made regarding the performance of specimens using the standard loading protocol versus the near-fault loading protocol [Yu et al, 1999]. This paper will focus on the plastic rotation, energy dissipation, and failure mode of RBS moment connections.

SPECIMEN DESIGN AND FABRICATION

Four nominally identical specimens, designated LS-1 through LS-4, were designed, constructed, and tested using the setup shown in Fig. 1. For LS-4 there was an added lateral brace 6 in. from the RBS region. The design, incorporating a reduced beam section, was based on a procedure recommended by Engelhardt [Engelhardt, 1998] and the AISC Seismic Provisions [AISC, 1997]. The RBS moment connection is illustrated in Fig. 2.

The specimens were fabricated and constructed by commercial companies. To simulate field conditions, the beam was installed and the moment connection welded with the column in an upright position. All welding was performed with the self-shielded flux-cored arc welding process, using electrodes that had a specified minimum

[1] *Associate Professor, University of California at San Diego, La Jolla, CA 92093-0085, USA Email:cmu@ucsd.edu*
[2] *Design Engineer, Degenkolb Engineers, 225 Bush St., San Francisco, CA 94104, USA Email: kyu@degenkolb.com*
[3] *Graduate Research Assistant, University of California at San Diego, La Jolla, CA 92093-0085, USA Email:cgilton@ucsd.edu*

Charpy V-Notch impact value of 20 ft-lbs at -20°F. The E71T-8 (0.072 in. diameter Lincoln NR-232) electrode was used for the complete joint penetration groove weld between the beam web and column flange, and the E70T-6 (3/32 in. diameter Lincoln NR-305) electrode was used for the welds between the beam and column flanges. The steel backing was removed from the beam bottom flange and the weld cleaned and covered with a fillet weld from below. The steel backing was left on the beam top flange, but a fillet weld was applied between it and the column flange.

Each specimen was made of A572 Grade 50 steel with special requirements (now called A992 Grade 50) per AISC Technical Bulletin [AISC, 1997]. The columns of specimens LS-1, LS-2, and LS-3 were from the same heat of steel, but the column of specimen LS-4 was from another heat. All four beams were from the same heat of steel. Tensile coupons were cut from the various shapes and tested according to ASTM standard procedures, with the results shown in Table 1. The values from the certified mill test reports are also included in Table 1.

LOADING HISTORIES

The standard SAC loading history in Fig. 3(a), developed by Krawinkler [SAC/BD-97/02, 1997], was used for Specimens LS-1 and LS-4. The loading sequence is controlled by inter-story drift angle, beginning with six cycles each of 0.375%, 0.5%, and 0.75% drift, sequentially. The next four cycles are at 1% drift, followed by two cycles of 1.5% drift. The sequence then completes two cycles each of successively increasing drift percentages (i.e., 2%, 3%, 4%, …) until failure.

The near-fault loading history (also developed by Krawinkler) used for Specimen LS-3 is presented in Fig. 3(b). The sequence begins with a pull to –2% drift, followed by a large push up to +6% drift (pull is hogging moment and push is sagging moment). There are then cycles between +1% and +5% drift, narrowing to cycles between +2% and +4% drift, and again up to +6% drift. The sequence then pulls across zero to –2% drift, back up to +3% drift, and back down to –1% drift. Finally, there are several cycles between +3% and 0% drift, narrowing to between +2% and 0% drift, before repeating. The same loading history was used for Specimen LS-2, but with the sign convention reversed.

TEST RESULTS

Specimens LS-1 and LS-4: Standard Loading Protocol

Specimen LS-1 performed well, remaining elastic through the cycles of 0.75% inter-story drift. Panel zone yielding began at 1% drift and minor local buckling was observed as early as 1.5% drift. Significant buckling began during the cycles of 3% drift, with lateral-torsional buckling (LTB) and web local buckling (WLB) measured at 3-1/4 in. and 1-3/16 in., respectively. By the second cycle at 4% drift (see Fig. 5) the LTB had increased to 4-1/2 in., the WLB increased to 2-13/16 in., and the strength degraded to just below 80% of the plastic moment capacity of the unreduced section. The test was halted after the third cycle of 5% drift due to strength degradation below 50% of the plastic moment capacity of the unreduced section. Fig. 4(a) is a plot of the load versus the displacement at the beam tip.

Specimen LS-4 behaved very similar to LS-1 up to 3% story drift ratio. After the second cycle of 3% drift LTB and WLB were measured at 3-1/16 in. and 1-1/8 in., respectively. Beyond 3% drift, the lateral bracing reduced the buckling amplitudes. At the end of the 4% drift cycles LTB and WLB had increased to only 3-1/2 in. and 2-3/8 in., respectively, and the strength had not significantly degraded. The testing continued through the 5% drift cycles and was stopped during the first cycle of 6% drift because of a failure in the bracing system. Fig. 4(d) is a plot of the load versus the beam tip displacement. A comparison of Figs. 4(a) and 4(d) shows the beneficial effect of providing lateral bracing near the RBS region to reduce the rate of strength degradation.

Specimens LS-2 and LS-3: Near-fault Loading Protocol

Specimen LS-2 exhibited excellent performance under the near-fault loading history. Panel zone yielding was noticed during the first excursion to +2% drift. Significant buckling of the beam bottom flange was observed during the following excursion to –6% drift, with LTB reaching 3-1/2 in., WLB reaching 2-1/16 in., and flange local buckling (FLB) reaching 1-7/16 in. During the following cycles to smaller inter-story drifts, the buckling amplitudes decreased. At the second –6% drift peak (see Fig. 6), the LTB, WLB, and FLB reached 3-7/8 in., 2-3/8 in., and 1-15/16 in., respectively. The following peak, +2% drift, saw a decrease in the buckling of the bottom flange and significant yielding of the top flange. During the following cycles the buckling amplitudes stayed within a range just below the values of the initial buckling. The loading history was repeated. At the

large peak of –6% drift the buckling continued to increase and a few cycles later fissure-like cracks were observed on the beam bottom flange near the RBS region. The loading history was completed again and started over. Soon after the initial –6% drift peak (the fifth time) the crack had propagated through half of the flange and the test was stopped. See Fig. 4(b) for a plot of the load versus the beam tip displacement.

The performance of LS-3 was very similar to that of LS-2. Panel zone yielding and significant buckling of the beam top flange near the RBS region occurred in the first two peaks. The recorded buckling amplitudes were somewhat higher than before, but the pattern was the same. After the second +6% drift LTB was 4-1/2 in., WLB was 2-3/8 in., and FLB was 2-3/8 in. Fissures were noticed around the third +6% peak and the beam top flange fractured just after the fourth due to low-cycle fatigue. See Fig. 4(c) for a plot of the load versus the displacement of the beam tip. Both near-fault specimens experienced low-cycle fatigue fracture in the RBS region. In reality this is unlikely to occur because of the short duration of near-fault ground motions.

RESPONSE COMPARISON

Plastic Rotation

Plots of the total plastic rotation versus the moment at the column face are included in Fig. 7. LS-1 and LS-4 both reached a total plastic rotation over 0.03 radian. The panel zone of each attributed to less than 0.01 radian. LS-2 and LS-3 reached total plastic rotations of 0.05 radian each. The panel zone of LS-2 attributed to less than 0.015 radian and the panel zone of LS-3 to less than 0.01 radian. The plastic rotation of the near-fault specimens (LS-2 and LS-3) was limited by the imposed displacement. Since neither specimen showed significant strength degradation, a higher plastic rotation (say, twice the plastic rotation of a specimen tested under a standard loading protocol) could have been achieved had a larger displacement been imposed. Clearly, the RBS connection can deliver a large plastic rotation to accommodate the deformation demand of a near-fault earthquake.

Energy Dissipation

Fig. 8 presents the amount of energy dissipated by each specimen, as well as the contributions of the beam and panel zone, separately. It can be seen that the majority of energy dissipation took place in the beam, at the RBS region. For LS-1 the beam dissipated 80% of the total energy dissipated by the connection, while the beam of LS-4 contributed 73% of its total energy dissipation. The beams of LS-2 and LS-3 dissipated 85% and 90%, respectively, of the total energy dissipated by the connections. All four specimens dissipated enough energy in the beam to prevent the brittle fracture of the flange groove welds. The average energy dissipation capacities for the standard and near-fault loading protocols were about the same.

Buckling Amplitude

A comparison was made of the buckling amplitudes of each specimen at each level of inter-story drift (Fig. 9). Specimen LS-4 was not included because of the added lateral bracing. From the figure it can be seen that the specimen tested with the standard loading protocol experienced higher buckling amplitudes at 5% drift than the specimens tested with the near-fault protocol experienced at 6% drift. Considering web local buckling, the buckling amplitude of LS-2 at 6% drift was half that of LS-1 at 5% drift. Similarly, the buckling amplitude of LS-3 at 6% was only three-quarters that of LS-1 at 5% drift.

CONCLUSIONS

Based on the test results of the four RBS moment connection specimens, the following conclusions can be made:

1. The seismic performance of the reduced beam section moment connection is excellent. No weld fracture was observed for any specimen. All specimens tested reached over the acceptable 0.03 radian plastic rotation, with the near-fault specimens reaching 0.05 radian. It is expected that with increased deformation demand, a specimen subjected to near-fault loading could develop twice the plastic rotation capacity it would develop under standard loading.

2. When LS-2 and LS-3 were repeatedly experienced to the near-fault loading protocol, they experienced beam flange fracture due to low-cycle fatigue. In reality, near-fault earthquakes will characteristically have a short duration, and low-cycle fatigue fracture is not likely to occur.

3. The energy dissipation capacities of the steel RBS specimens were insensitive to the different types of loading protocols experienced.

4. Buckling amplitudes for the near-fault specimens were lower than those of the standard specimens at comparable drift levels.

ACKNOWLEDGEMENTS

This testing program was sponsored by the SAC Joint Venture with Mr. Jim Malley as the Project Director for Topical Investigations. The authors would like to thank PDM/Strocal, Asbury Steel, TSI Inc., AISC, and the Northridge Steel Industry Fund for their contributions to this project.

REFERENCES

Chen, S.-J., Yeh, C. H., and Chu, J. M., (1996) "Ductile Steel Beam-to-column Connections for Seismic Resistance," *J. Struct. Engrg.*, Vol. 122, No. 11, pp. 1292-1299, ASCE.

Clark, P., Frank, K., Krawinkler, H., and Shaw, R., (1997) "Protocol for Fabrication, Inspection, Testing, and Documentation of Beam-Column Connection Tests and Other Experimental Specimens," *Report No. SAC/BD-97/02*, SAC Joint Venture, Sacramento, CA.

Engelhardt, M. D., (1998) "Design of Reduced Beam Section Moment Connections," *1999 North American Steel Construction Conference Proceedings*, pp. 1-3 to 1-29, AISC.

Engelhardt, M. D., Winneberger, T., Zekany, A. J., and Potyraj, T., (1998) "Experimental Investigation of Dogbone Moment Connections," *Engineering Journal*, Vol. 35, No. 4, Fourth Quarter, pp. 128-139, AISC.

Plumier, A., (1997) "The Dogbone: Back to the Future," *Engineering Journal*, Vol. 34, No. 2, pp. 61-67, AISC.

Seismic Provisions for Structural Steel Buildings (1997), 2nd Edition, AISC, Chicago, IL.

"Shape Material (ASTM A572 Gr. 50 with Special Requirements)," *Technical Bulletin No. 3* (1997), AISC, Chicago, IL.

Yu, Q. S., Gilton, C. S., Uang, C.-M., (1999) "Cyclic Response of RBS Moment Connections: Loading Sequence and Lateral Bracing Effects," *Report No. SSRP 99-13*, University of California at San Diego, La Jolla, CA.

Zekioglu, A., Mozaffarian, H., Chang, K. L., Uang, C.-M., and Noel, S., (1997) "Designing After Northridge," *Modern Steel Construction*, Vol. 37, No. 3, pp. 36-42, AISC.

Table 1: Mechanical Properties

Specimen	*Member*	*Coupon*	F_y *(ksi)*	F_u *(ksi)*	*Elongation (%)*
All	Beam W30×99	Flange	55	72	28
		Web	58	75	26
		(Mill Cert.)	(56)	(74)	(26)
LS-1,2,3	Column W14×176	Flange	56	74	31
		Web	54	73	28
		(Mill Cert.)	(58)	(76)	(21)
LS-4	Column W14×176	Flange	-	-	-
		Web	-	-	-
		(Mill Cert.)	(64)	(84)	(26)

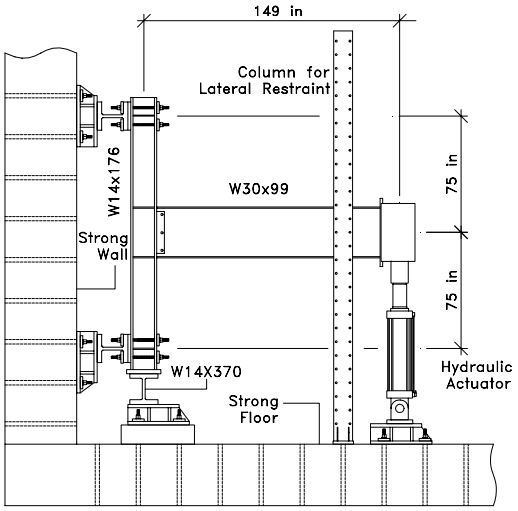

Figure 1: Test Set-up

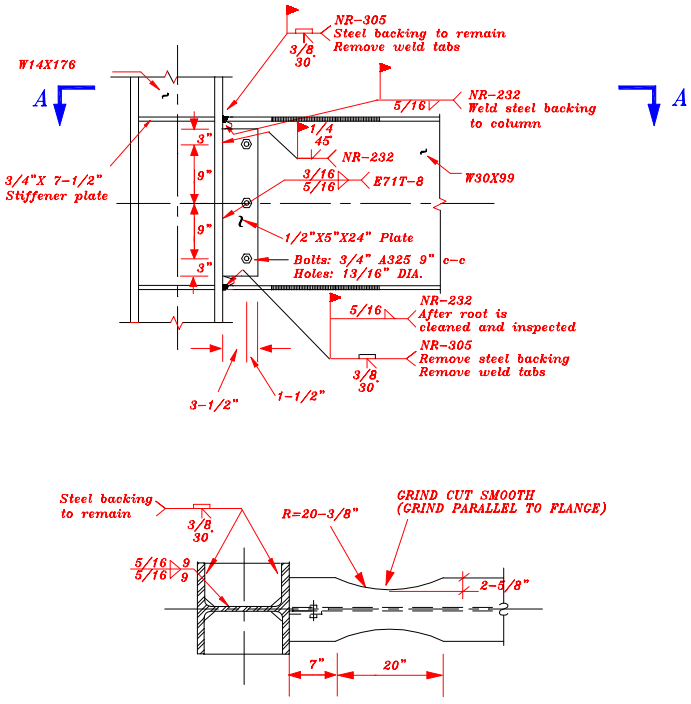

Figure 2: Connection Detail

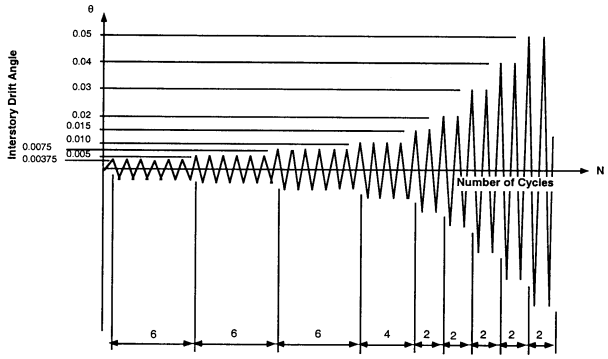

(a) Standard Loading Protocol

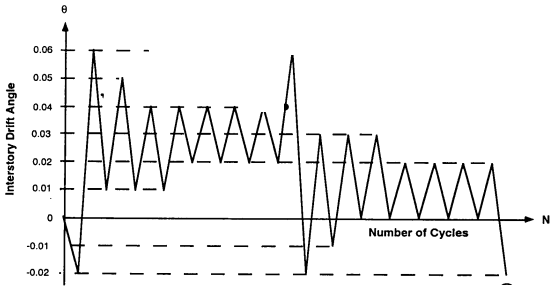

(b) Near-fault Loading Protocol

Figure 3: Loading Histories

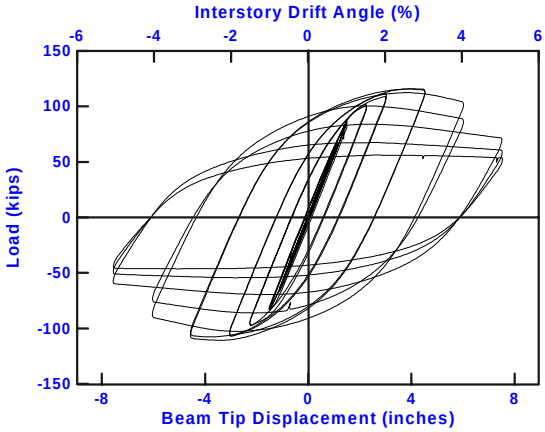

(a) LS-1

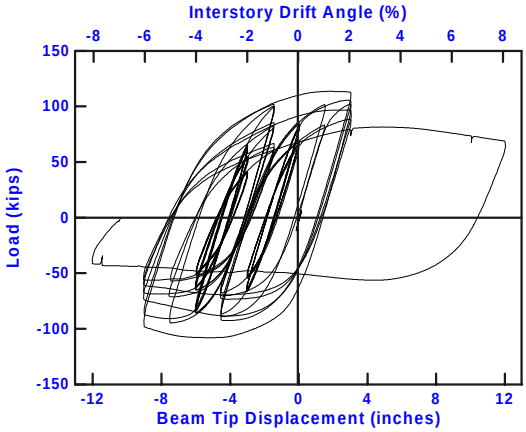

(b) LS-2

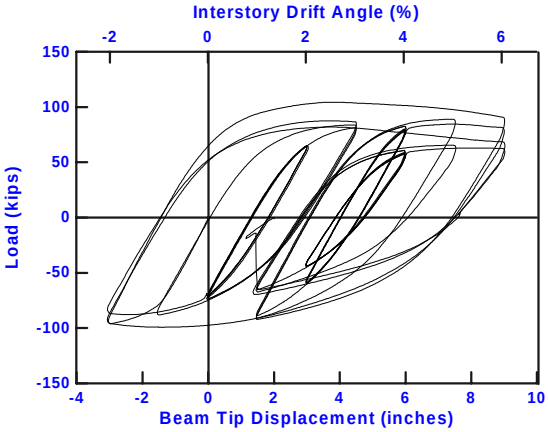

(c) LS-3

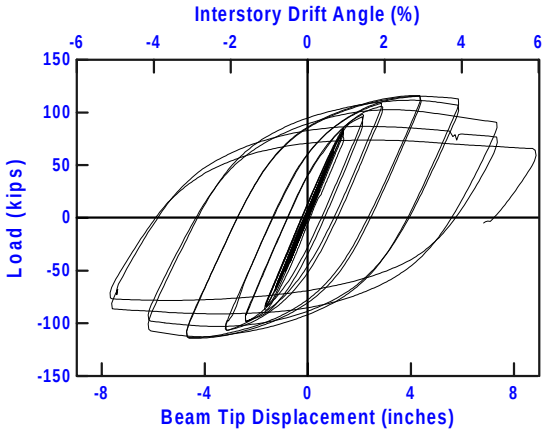

(d) LS-4

Figure 4: Load versus Beam Tip Displacement Relationships

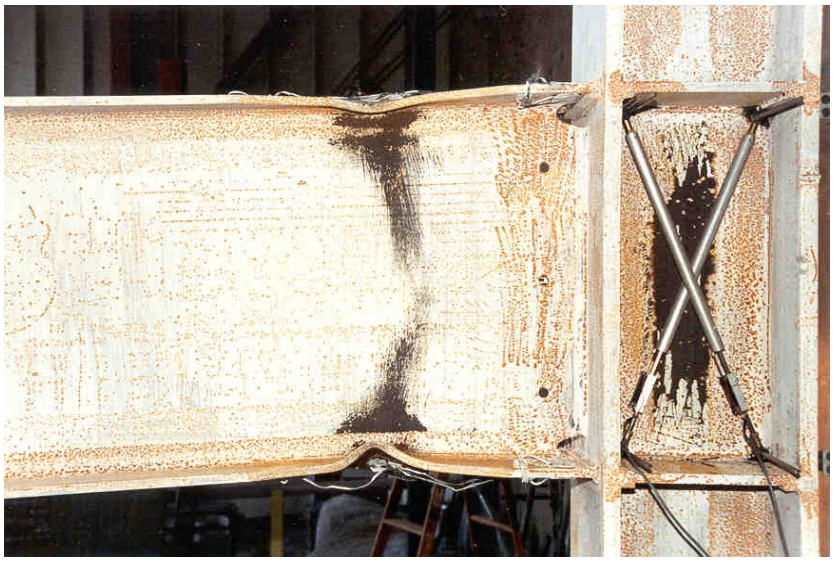

Figure 5: Yielding and Buckling Pattern of LS-1 at –4% Drift

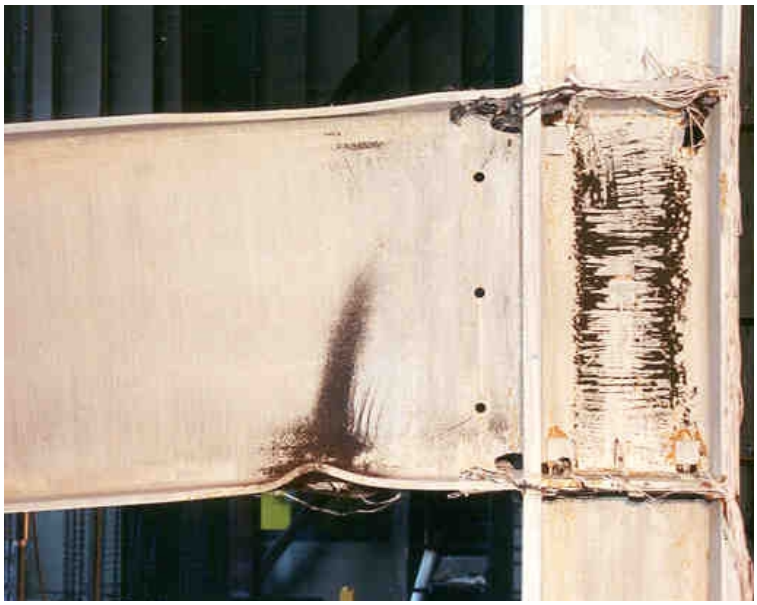

Figure 6: Yielding and Buckling Pattern of LS-2 at Second –6% Drift Peak

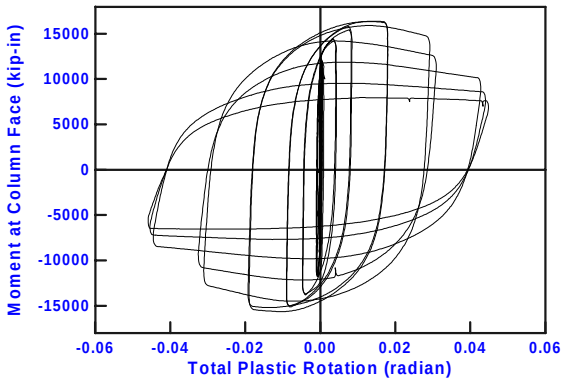

(a) LS-1

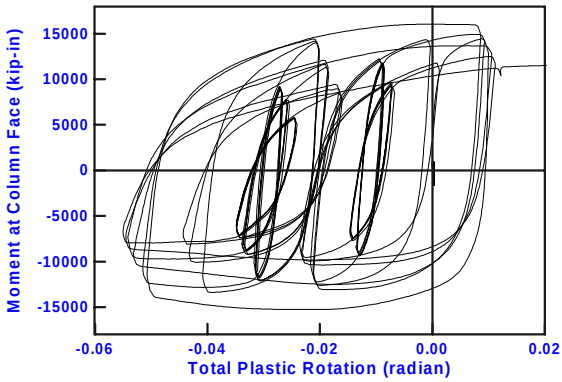

(b) LS-2

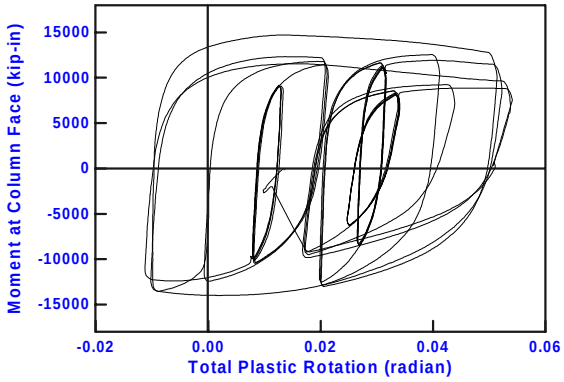

(c) LS-3

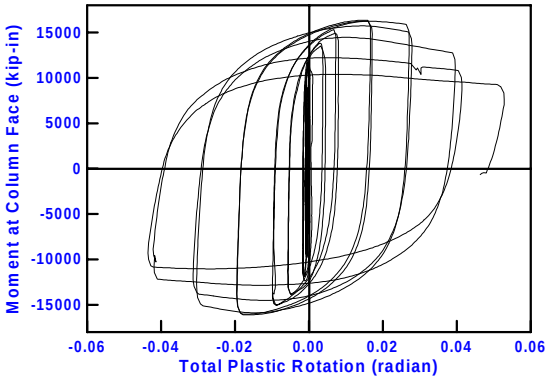

(d) LS-4

Figure 7: Moment versus Total Plastic Rotation